White Rose Research Online

eprints@whiterose.ac.uk
https://eprints.whiterose.ac.uk
Universities of Leeds, Sheffield and York

Deposited via The University of Leeds.

White Rose Research Online URL for this paper:
https://eprints.whiterose.ac.uk/id/eprint/168537/

Version: Accepted Version

Article:
Jayathilaka, P, Indraratna, B and Heitor, A (2021) Influence of Salinity-Based Osmotic Suction on the Shear Strength of a Compacted Clay. International Journal of Geomechanics, 21 (5). 04021041. ISSN: 1532-3641

https://doi.org/10.1061/(ASCE)GM.1943-5622.0001988

© 2021 American Society of Civil Engineers. This is an author produced version of an article published in International Journal of Geomechanics. Uploaded in accordance with the publisher's self-archiving policy. This material may be downloaded for personal use only. Any other use requires prior permission of the American Society of Civil Engineers. This material may be found at https://doi.org/10.1061/(ASCE)GM.1943-5622.0001988

Reuse
Items deposited in White Rose Research Online are protected by copyright, with all rights reserved unless indicated otherwise. They may be downloaded and/or printed for private study, or other acts as permitted by national copyright laws. The publisher or other rights holders may allow further reproduction and re-use of the full text version. This is indicated by the licence information on the White Rose Research Online record for the item.

Takedown
If you consider content in White Rose Research Online to be in breach of UK law, please notify us by emailing eprints@whiterose.ac.uk including the URL of the record and the reason for the withdrawal request.

UNIVERSITY OF LEEDS
University of Sheffield
UNIVERSITY of York

INFLUENCEOFSALINITY BASED OSMOTIC SUCTION ON THE SHEAR STRENGTH OF A COMPACTED CLAY

PubuduJayathilaka

PhD student,

Centre for Geomechanics and Railway Engineering, University of Wollongong,

NSW 2522, Australia

Buddhima Indraratna[1]

Distinguished Professor of Civil Engineering,

Director, Transport Research Centre, University of Technology Sydney, Australia

Formerly, Director, Australian Research Council (ARC) Industrial Transformation Training Centre, ITTC-Rail, University of Wollongong, Australia

Ana Heitor

School of Civil Engineering, University of Leeds, Leeds, UK

Formerly Centre for Geomechanics and Railway Engineering, University of Wollongong,

NSW 2522, Australia

Words: 6584; Figures: 14

Submitted to:

[1]Corresponding author: Prof Buddhima Indraratna

Email: buddhima.indraratna@uts.edu.au

ABSTRACT

As most previous studies have neglected the positive influence of salinity (osmotic suction) on most coastal soils in Australia, the design of transport infrastructure involving these soils have often been overly conservative. In this study, a laboratory approach based on direct shear testing is explained to determine the stress-strain behaviour of compacted coastal silty clay (CL) at different levels of osmotic suction generated by varying salinity (NaCl) concentrations. A broad data set for a total of 147 direct shear tests conducted on remoulded and re-compacted test specimens at seven different initial matric suction conditions is analysed to develop a semi-empirical model that captures the effect of osmotic suction on the soil shear strength. The results suggest that greater the initial matric suction is the more pronounced will be the role of osmotic suction. The proposed semi-empirical model is governed by an electrical conductivity relationship with the osmotic suction generated by soil salinity. A new parameter χ_2 is introduced to quantify the role of soil salinityon the apparent soil shear strength corresponding to different levels of osmotic suction. When this novel relationship is coupled with the conventional matric suction theory, the overall unsaturated shear strength of a saline soil can be properly evaluated, as proven by the close proximity of the predictions to the measurements.

Keywords: Unsaturated, matric suction, osmotic suction, shear stress

INTRODUCTION

Most types of civil infrastructure are built on and remainunder unsaturated conditions for most of their service life; therefore, the stability of these structures with increased loading in the future will depend on the actual shear strength of the foundation soil (sub-grade). Especially in notably saline soils prevalent along the coastal belt of Australia, neglecting the benefits of salinity-based osmotic suction can lead to undue design conservatism. Past studies have shown that the magnitudes of both matric and osmotic suction influence the shear strength of a natural or compacted soil (Graham et al., 1992, Barbour and Fredlund, 1989). However, while the effect of matric suction on the shear strength is well established through comprehensive testing and analysis (Khalili, 2018, Vanapalli et al., 1996, Bishop, 1960, Khalili et al., 2004), only a limited number of studies have focussed on the role of osmotic suction. For instance, Tiwari and Ajmera (2014), Xu (2019), and Di Maio and Scaringi (2016)verified the corresponding increase in soil shear strength as the osmotic suction is increased. Fredlund et al. (2012) pointed out that osmotic suction would have greater influence at higher values of matric suction, hence a key reason why the authors in the current study have investigated the role of osmotic suction at different levels of matric suction for a coastal saline soil. Elsewhere in relation to plant morphology, Pathirage et al. (2017) and Jayathilaka et al. (2019) have pointed out that the variations of soil osmotic suction can also be associated with the nutrient uptake by roots; this effect is not considered in this study.

Osmotic suction stems from the salts dissolved in the pore water of a soil, and particularly in coastal areas salinity is significantly increased by sodium chloride (NaCl) that is transported and deposited in inland areas over the geological time domain, i.e. in some instances, even several thousands of km away from the present-day marine boundary. Arora (2017) reports

47 that around 400 million hectares, which is more than 6% of the total landmass of the earth
48 can be categorised as saline, while in Australia alone, about 30% of its landmass is
49 considered to be saline (Rengasamy, 2006).

50 The soil strength is influenced by the degree of saturation, the presence of various chemical
51 compounds, the overburden and confining ground pressure, and the fabric of the soil and pore
52 water conditions that also influence the inter-particle behaviour(Murray and Sivakumar,
53 2010). The osmotic suction induced by variations in pore water salinity can induce
54 inter-particle forces, e.g. van der Waal attraction forces, electrostatic repulsive forces, and
55 surface hydration forces (Li et al., 2013). While some of these stress components can help to
56 reduce potential swelling (Rao and Thyagaraj, 2007), as the osmotic suction changes, the
57 hydraulic and mechanical properties of a compacted soil also contribute to the thinning of the
58 diffusive double layer (DDL), cause the particles to coagulate, and increase the effective
59 stress (Di Maio et al., 2004). While the effective pressure acting on clay particles can be
60 described for instance by Derjaguin-Landau-Verwey-Overbeek (DLVO) theory of stability
61 (Liang et al., 2007), determining the magnitudes of these inter-particle forces through
62 accurate measurements is still a challenge(Fredlund et al., 2012). Electrical conductivity is
63 widely used in geophysical applications (Shevnin et al., 2010, Jiao-Jun et al., 2007, Shah and
64 Singh, 2004), while its ability to corroborate with matric suction (Hen-Jones et al., 2014,
65 Piegari and Maio, 2013) and osmotic suction (Adam et al., 2012, Read and Cameron, 1979)
66 has been widely tested and discussed. Nevertheless, the combination of electrical
67 conductivity and osmotic suction to predict the soil shear strength is still at infancy.

68 In view of the above, a novel osmotic stress parameter (χ_2) is introduced in this paper to
69 determine the stress induced by changes in osmotic suction attributed to different salt
70 concentrations in the pore water. The role that osmotic suction plays in the shear strength of a

71 soil compacted at different levels of matric suction is then investigated through a series of
72 direct shear tests.

73 OSMOTIC STRESS PARAMETER

74 A new shear strength model which can capture the influence of both the matric and osmotic
75 suction on the shear strength is introduced in this paper. Here, the shear strength of the soil
76 with pore water salinity can be partially related to the saturated shear strength parameters
77 based on the traditional effective cohesion (c') and effective friction angle (ϕ'). In addition,
78 instead of the effective stress parameter (χ_1) proposed by Khabbaz and Khalili (1998), a
79 revised osmotic stress parameter (χ_2) that depends on the level of salinity in pore water is
80 introduced as follows:

$$\sigma_{net} = (\sigma_N - u_a) + \chi_1(u_a - u_w) + \chi_2\pi \quad (1)$$

81 In the above, the term $(\sigma_N - u_a)$ is the effective normal stress, σ_N is the total normal stress,
82 the parameter $\chi_1 = \left(\frac{u_a - u_w}{AEV}\right)^{-0.55}$ is the effective stress parameter that depends on the matric
83 suction, the term $(u_a - u_w)$ is the matric suction, u_a is the pore air pressure, u_w is the pore
84 water pressure, AEV is the air entry value, and π is the osmotic suction.

85 Equation (1) conforms with the postulate that the inter-particle physio-chemical stresses can
86 be superimposed directly to the classical effective stress concept (Lu & Likos 2006; Rao &
87 Thyagaraj 2007). Also as proposed earlier by Lu and Likos (2006), the net inter-particle
88 contact forces due to physico-chemical effects can be determined by the summation of
89 chemical cementation (bond stresses), van der Waals attraction forces, and the repulsion
90 forces of DDL. Therefore, by characterising χ_2 in terms of inter-particle contact, the relevant
91 forces are more realistically acknowledged, but as noted by Fredlund et al. (2012), the

methods of determining or measuring the correct magnitude of the aforementioned inter-particle contact forces remains a challenge.

EXPERIMENTAL DETERMINATION OF χ_2

According to Khabbaz and Khalili (1998), the shear strength of unsaturated soil can be estimated in terms of the effective normal stress $(\sigma_N - u_a)$ and matric suction $(u_a - u_w)$:

$$\tau'_U = [(\sigma_N - u_a) + \chi_1(u_a - u_w)] \tan \phi' + c' \quad (2)$$

Where, τ'_U is the unsaturated shear strength, σ_N is the total normal stress, u_a is the pore air pressure, u_w is the pore water pressure, $\chi_1$is the effective stress parameter that depends on the matric suction, ϕ' is the effective friction angle, and c' is the effective cohesion component. Since the effective stress generated in an unsaturated soil element is defined by considering the net stress constituting the pore water and pore air pressures, pore water salinity (hence, the matric and osmotic suction, and physio-chemical pressure), it is assumed that the shear strength parameters c' and ϕ' of saturated soil are independent of the matric suction (Khabbaz and Khalili, 1998) and of the salinity-based osmotic suction (Lu and Likos, 2006). Combining these concepts in a mathematical sense, a refined shear strength model for unsaturated-osmotic conditions is now defined by the following expression:

$$\tau'_{US} = [(\sigma_N - u_a) + \chi_1(u_a - u_w) + \chi_2\pi] \tan \phi' + c' \quad (3)$$

Where τ'_{US} is the shear strength of osmotically induced unsaturated soil.The difference between Equations (2) and (3) is given by the osmotic suction component as follows:

$$\tau'_{US} - \tau'_U = \chi_2\pi \tan \phi' \quad (4)$$

110 Hence, according to Equation (4), the only unknown parameter χ_2 can be estimated.

$$\chi_2 = \frac{\tau'_{US} - \tau'_U}{\pi \tan \phi'} \tag{5}$$

111 RELATIONSHIP BETWEEN χ_2 AND THE ELECTRICAL CONDUCTIVITY RATIO

112 Electrical conductivity is a function of the salt concentration so it can also be considered as a
113 function of osmotic suction (Abedi-Koupai and Mehdizadeh, 2007). To investigate the
114 behaviour of χ_2 the electrical conductivity of soil is used as an additional influencing factor.
115 A semi-empirical model parameter (i.e. χ_2) is introduced based on the experimental results.
116 In this model, ECR is used to represent the change of salinity in pore water and S_r is used to
117 incorporate the influence of the degree of saturation.

$$\chi_2 \begin{cases} = 0 & \pi = 0 \\ = \dfrac{a}{S_r^c}\left(1 - \exp\left(-b(ECR)\right)\right) & \pi \neq 0 \end{cases} \tag{6}$$

118 In the above, the electrical conductivity ratio $(ECR) = \frac{\Delta EC}{EC_i}$, $\Delta EC = (EC - EC_i)$, EC is the
119 electrical conductivity of the saturated soil for a given salt concentration in pore water, EC_i is
120 the initial electrical conductivity of saturated soil remoulded with distilled water, S_r is the
121 degree of saturation, and a, b and c are empirical coefficients from the regression analysis of
122 experimental results.

123 The sensitivity of χ_2 depends mainly on the above three experimental coefficients, and their
124 influence on χ_2 is shown in Fig. 1. The coefficient a increases to the maximum of χ_2,
125 however, coefficient b does not influence the maximum value of χ_2, but rather contributes to

126 the lowest value of ECR having the maximum χ_2. The maximum theoretical value of χ_2 can
127 then be calculated from Equation (7).

$$\chi_{2max} = (\frac{a}{S_r^c}) \quad (7)$$

128 According to Equation (7), $\chi_{2_{max}}$ does not depend on the electrical conductivity ratio (ECR),
129 although χ_2 is a function of ECR. This is further validated by Fig. 1(d) which shows the
130 distribution of χ_2 with respect to ECR for different $\frac{a}{S_r^c}$ratios. According to Fig. 2, the
131 distribution of $\chi_{2_{max}}$ with respect to the empirical coefficient *c* is linear at higher degrees of
132 saturation, but the distribution of $\chi_{2_{max}}$ becomes exponential as the degree of saturation
133 decreases. Therefore, at higher matric suctions (i.e. lower degree of saturation), the influence
134 of χ_2 will be significant compared to that of a soil having a lower soil matric suction (high
135 degree of saturation).

136 The minimum ECR value where χ_2 reaches its maximum and the critical ECR (i.e. ECR_C)
137 depends on the empirical coefficient *b*[Fig. 1(b)], therefore, $\chi_{2_{max}}$ increases as the soil
138 approaches a dry state. The distribution of ECR_C with respect to the empirical coefficient *b*
139 for different levels of saturationis shown in Fig. 3. Here, for every degree of saturation, the
140 ECR_C decreases as the coefficient *b*increases, following a power decay function. For
141 example, under fully saturated conditions (S_r = 1), when the coefficient *b* increases from 0.01
142 to 0.08, the ECR_C decreases from 750 to 125.

MATERIALS AND TESTING PROGRAM

Soil type and preliminary testing

The soil samples were obtained from the coastal region of Wollongong (85 km south of Sydney). The particle size distribution (AS1289.3.6.1) indicates it consists of sand (48%), silt (36%), and clay (16%) particles (Fig. 4). The liquid and plastic limits (AS1289.3.1.1 and AS1289.3.2.1) are 46.8% and 27.7%, so this soil can be classified as a sandy, silty clay of low plasticity, CL, based on the ASTM Unified soil classification (ASTM D2487 2010). The modified Proctor compaction characteristics according to AS1289.5.1.1 enabled a maximum dry density (MDD) of 15.58 kN/m^{3}at an optimum moisture content of 27.2%, and a specific gravity of the soil was determined to be 2.62 (AS1289.3.5.2).

The matric suction of the compacted soil was measured using the contact method and Whatman No 42 filter paper approach (ASTM D5298-03). The soil water retention data was only measured for test specimens remoulded with distilled and de-aired water. Thirteen different samples were prepared at different moisture contents, and then they were air sealed and stored for seven days in a temperature and humidity controlled room (20±2^{o}C, 30%RH) to attain moisture equilibrium. The samples were then compacted into a 50mm diameter cylindrical mould to 85% of MDD. Fig. 5 shows the soil water retention curve calibrated with the Van Genuchten (1980) model (Van Genuchten 1980) withbest-fit parameters: m=0.306, n=1.44, and α=0.008.

Although, the osmotic suction can be theoretically calculated according van Hoff's equation ($\pi = \upsilon R^* TC$), where π is the osmotic suction, R^* is the universal gas constant, T is the absolute temperature, υ is the valency, and C is the ion concentration. In this study, the actual

165 osmotic suction was measured using a WP4 Dew Point Potentiometer. Crystallised NaCl
166 were mixed with distilled water to prepare a solution with the desired salt concentrations.
167 Although the soil contains constant ion content, the pore water salinity is likely to increase
168 due to soil moisture decrease (i.e. caused by a rise in global temperature induced by climate
169 change). Therefore, it is appropriate to consider a broader range of salinity values. Therefore,
170 seven soil samples were fully saturated with solutions having NaCl concentrations of 0.0, 0.2,
171 0.4, 0.6, 0.8, 1.0 and 2.0 mol/L, where the maximum salinity of the studied soil was three
172 times more than the maximum salinity of seawater (i.e. 35 g/L). Also, the inherent salt
173 content of the soil specimen was determined by X-Ray diffraction (XRD) as less than 0.1%.
174 Therefore, for this study, the contribution of inherent salt content could be assumed as
175 negligible. The samples were then fully sealed and stored in a temperature and humidity
176 controlled room (20±2^{o}C, 30% RH) for another 24 hours. Although the WP4C Dew Point
177 Potentiometer could be used to measure total suction, in this study, as the seven test
178 specimens remained fully saturated the matric suction was 0 kPa. On this basis, the measured
179 total suction was assumed to be equal to the osmotic suction of the specimen. The moisture
180 equilibrated samples were placed into clean plastic cups and tested with a WP4C Dew Point
181 Potentiometer (range 0 to 300 MPa). The measured values of osmotic suction are summarised
182 in Table 1.

183 Seven samples saturated with different pore water salinities were prepared and stored in the
184 temperature and humidity-controlled room for 24 hours. These moisture equilibrated samples
185 were then compacted to a dry density of 13.24 kN/m^3 (85% of MDD) and then placed into a
186 standard electrical resistivity measuring box having dimensions of 38 x 101.5 x 152.3 mm.
187 The electrical resistivity was measured using a Tinker and Rasor SR-2 soil resistivity meter
188 (±0.1 Ωcm accuracy) and then converted to electrical conductivity (=1/Electrical resistivity).

189 The distribution of electrical conductivity with the pore water saline concentration is
190 summarised in Fig. 6.

191 **Direct shear test**

192 Seven different solutions with different osmotic suctions were prepared by mixing the
193 relevant amount of commercially available crystallised NaCl with distilled water; only NaCl
194 was used to mimic the conditions of coastal soils. Different levels of initial matric suction
195 (0, 25, 100, 200, 500, 1000 and 1500 kPa) were targeted by controlling the moisture content
196 of the specimens. The required amount of water and the relevant salt concentration were
197 added to the soil, and then the mixture was left in the temperature and humidity-controlled
198 room for seven days for chemical and moisture equilibration. The samples were then
199 compacted in a 60×60×40 mm shear box chamber to attain 85% of MDD, and then stored in
200 the temperature and humidity-controlled room for two more days.

201 A motor-driven direct shear box where the specimen carriage travels on roller bearings was
202 used to maintain a constant rate of horizontal displacement of 0.006 mm/min. A load cell and
203 two LVDT transducers accurate within ±0.001 kN,±0.001mm and ±0.001 mm, respectively,
204 were used to determine the horizontal shear force, vertical displacement, and horizontal
205 displacement. A lever arm loading system (beam ratio 10:1) was used to apply a vertical load
206 by a top cap modified to accommodate a miniature pore water pressure transducer, so that
207 any variations in the matric suction could be monitored during shearing. An in-house coded
208 program with Lab VIEW software complemented by a National Instruments card
209 (NI USB-6009) with eight input channels was used to acquire data every 60 seconds. A
210 schematic diagram and few images of the actual test set up of the direct shear box are given
211 in Fig. 7.

212 Apart from those specimens with a matric suction of 0 kPa (fully saturated conditions), direct
213 shear tests were carried out at different levels of matric suction under constant water (CW)
214 contents. For fully saturated experiments where the matric suction = 0 kPa, the compacted
215 specimens were fully submerged in the desired saline solution for 24 h before shearing to
216 attain moisture and chemical equilibration. To ensure CW conditions, evaporation from the
217 soil specimen had to be minimised so the compression and shearing stages of the direct shear
218 tests could occur within a temperature and humidity-controlled environment. The top and
219 bottom surfaces of all test specimens were covered with a 1mm thick film of polyethylene to
220 minimise evaporation. Moreover, the space between the top and bottom sliding halves, and
221 any other gaps between the top cap and bottom plate were sealed with silicon grease. The
222 volume of air around the specimen was reduced by enclosing the direct shear box and the
223 assembly inside an airtight polythene bag which was then covered with a damp cloth to
224 reduce any variations in temperature inside the polythene bag (Fig. 7). The moisture contents
225 of soil specimens before the compaction and after the direct shear test were determined.
226 However, the average moisture content variation was found to be negligible (< 0.1%).
227 Therefore, soil specimen was assumed to be at a constant water content condition during
228 compaction and shearing.

229 During the compression stage, the specimens were loaded vertically in 10, 20 and
230 40 kPa steps, where each load increment was left for one to two days until the variations of
231 vertical displacement became insignificant (<1%). The specimens were then sheared at a
232 relatively low shear strain rate of 0.006 mm/min, in order to accommodate the redistribution
233 of any variation in matric suction induced by the shearing process. Shearing continued until a
234 maximum shear strain of 25% was achieved.

235 RESULTS AND DISCUSSION

236 **Stress-strain behaviour**

237 The shear stress and strains of 147 soil samples were measured at three different normal loads
238 for given osmotic suctions and various initial matric suctions. Of those, the distributions of
239 shear stress and normal strain were plotted against the shear strain for different osmotic
240 suctions for fully saturated conditions. The stress-strain behaviour of the fully saturated soil
241 without the influence of salinity (π = 0 kPa), was determined to consider as a reference to
242 compare the stress-strain behaviour of the soil with variable osmotic suctions under
243 unsaturated conditions.

244 The saturated stress-strain behaviour of the soil for various osmotic suctions for a given
245 normal stress (σ'_N = 10 kPa) is shown in Fig. 8. The results show that the peak shear stress
246 increases gradually with the influence of osmotic suction, showing a maximum increase of
247 around 13.48 kPa. Moreover, the stress-strain behaviour of the unsaturated soil was
248 monitored for six different matric suction conditions as discussed above. Of those, the
249 stress-strain distribution for two different pressure conditions (different applied normal
250 stresses and matric suctions) is shown in Fig. 9. Similar to the behaviour of saturated soil, the
251 peak stress of unsaturated soil increases with osmotic suction. The reason for this is the
252 increased resistance for the relative movement of soil particles due to the increase in inter-
253 particle bond strength. However, the increase of peak shear stress of unsaturated soil with
254 respect to osmotic suction was higher compared to the saturated condition for a given normal
255 stress. For example, the soil specimen subjected to 1500 kPa matric suction shows an
256 increase of around 98.96 kPa of peak shear stress for the highest osmotic suction increase,
257 while the saturated soil shows only about 13.48 kPa for the same increase of osmotic suction.

Hence, it is evident that both matric suction (as expected) and osmotic suction has a significant influence on the peak shear stress.

The influence of osmotic suction on normal strain response of the saturated and unsaturated soil for a given normal stress is shown in Fig. 8 and 9. The results indicate that for all the osmotic and matric suction conditions, the normal strain decreases, showing a contractive behaviour of the specimens. Furthermore, an increase in osmotic suction results in lower contraction of the specimen for both saturated and unsaturated conditions. Also, as expected, at higher matric suctions the specimens exhibit a lower contraction behaviour compared to saturated conditions. This contractive behaviour of soil specimens can be further elaborated with maximum normal strain results. The maximum normal strain is considered as the lowest achieved normal strain of the specimen. The distribution of maximum normal strain with respect to osmotic suction for various matric suctions for a given normal stress (σ'_N = 10 kPa) is shown in Fig. 10. For all the matric suction conditions, the maximum normal strain significantly decreases with osmotic suction, showing the highest decrease of change of maximum normal strain of around 4.7%. This could be because of the increased resistance to the relative movement of particles due to the influence of osmotic suction. Further as expected, the change of maximum normal strain also decreases with matric suction. Interestingly, while the change of maximum normal strain without the influence of osmotic suction is around 2.7% (σ'_N = 10 kPa), at higher matric suctions (1500 kPa) the change of maximum normal strain decreases to 0.27% for the same increase of osmotic suction.

Model calibration and validation

The peak shear strength was determined from the results of the direct shear tests. The summary of all the peak stress results is given in Table 2. The experimental distribution of $\chi_2$was calculated based on Equation (5). The saturated friction angle was calculated when the soil sample became fully saturated with distilled water (π = 0 kPa). The unsaturated behaviour of soil is influenced by the level of matric suction. Therefore, the influence that the matric suction has on $\chi_2$was considered by incorporating the corresponding degree of saturation into Equation (6). Due to the limited available literature for this soil suction range, three independent data sets have been used for calibration (i.e. σ'_N = 20 kPa) and validation (i.e. σ'_N = 10 and 40 kPa). The proposed new model for χ_2 [Equation(6)] was calibrated for three major initial matric suction conditions such as s_i = 0 kPa (saturated), s_i = 200 kPaand 500 kPa, with respect to experimental results for a given normal stress (σ'_N = 20 kPa).The distribution of χ_2 with the electrical conductivity ratio for three different levels of matric suctions is shown in Fig. 11; it was used to estimate the best-fit parameters which were then used to predict the unsaturated behaviour of soil in combination with the degree of saturation for the other independent data sets. The fully saturated condition was used to determinethe*a* and *b* coefficients when the influence of *c*was not significant (S_r = 1). Then the parameter *c* was determined based on the results from s_i = 200 kPa condition, and also further calibrated all the three parameters with s_i = 500 kPa. Based on these determinations, the calibrated parameters are a = 0.003, b = 0.0375 and c = 2. The proposed model was validated for two independent loading conditions (σ'_N = 10 and 40 kPa) with the calibrated model parameters, and the corresponding validation results are shown in Fig. 12. In general, the model predictions match the experimental results very well, thus indicating that the proposed model incorporating$\chi_2$is able topredictthe osmotically induced shear strength of a saline soil.

303 The above results also show that χ_2 increases with an increasing ECR ($\Delta EC/EC_i$), but this
304 increase in χ_2 also decreased at high ECR values until it reached a maximum theoretical χ_2
305 value of 0.003 under saturated conditions irrespective of applied stress. The maximum
306 theoretical χ_2 increases as the initial degree of saturation decreases or the initial matric
307 suction increases. The minimum value of ECR where χ_2 reached its maximum or the critical
308 ECR (ECR_c), does not depend on the initial matric suction; hence it is evident that the ECR_c
309 is a parameter which only depends on the pore solution and surface potential of soil particles.

310 The predicted peak shear stress was calculated based on Equation (3) and the results were
311 compared with the experimental results for two independent applied normal stress conditions;
312 the corresponding distribution of model prediction and experimental results of peak shear
313 stress is shown in Fig. 13.The model predictions match the experimental results at lower
314 initial matric suctions (< 500 kPa), giving a maximum deviation of less than 5kPa. However,
315 as the initial matric suction (>500 kPa) increases, the model shows a slight deviation
316 (5 to 14.5 kPa) depending on the magnitude of osmotic suction and matric suction. Overall,
317 the model exhibits an increased deviation from the experimental results at the highest values
318 of osmotic suction and initial matric suction. The maximum deviation of model results from
319 experimental results for any condition is about 14.5kPa when the osmotic suction increases to
320 9560 kPa at the highest considered initial matric suction of 1500 kPa.

321 MODEL LIMITATIONS

322 The proposed unsaturated shear strength model was primarily based on the salinity level
323 (hence, osmotic suction) and the initial matric suction. The model was calibrated and
324 validated using the shear box results for a clayey soil of low plasticity (CL; PI=19) under
325 constant water content. The measured maximum matric suction changes upon shearing were

326 generally very small compared to the relatively high initial matric suction, as shown in
327 Fig. 14 for a typical test specimen. Therefore, while the proposed model is accurate under
328 these specific conditions, when considering its broader application to other soils, the
329 following limitations can be elucidated.

330 • This unsaturated shear strength model was validated only for a single soil of low
331 plasticity (CL). Therefore, the application of the model to soils of much higher
332 plasticity(e.g. CH, OH, MH) will require caution to be exercised.
333 • Duringshearing (constant water content) the pore structure (void ratio) can change
334 with an accompanied change in the degree of saturation. Fig. 14 shows for an initial
335 matric suction of 1500 kPa, the maximum change in matric suction upon shearing is
336 in the proximity of 35 kPa (< 2.5%). For soils of different fabric that significantly
337 dilate upon shearing(e.g. dense granular soils or highly compacted fills), the shearing-
338 induced matric suction changes may be large enough to induce notable discrepancies
339 of the proposed shear strength model.
340 • Under near saturation, the role of matric suction will be eliminated, hence the shear
341 strength parameter (χ_2) represented by Equation (6)becomes simplified as a sole
342 function ofsalinity. In this regard, further tests conducted at much greater osmotic
343 suction (e.g. in the proximity of say 100 MPa)will be desirable to calibrate$\chi_2$more
344 accurately.
345 • It is appreciated that remoulded soil specimens may not truly represent the actual
346 hydro-mechanical behaviour of in situ soil. However, due to technical difficulties in
347 obtaining many identical undisturbed test specimens (i.e. same microstructure and
348 pore water salinity), remoulded samples were used for this study.Undisturbed block

samples to fit the dimensions of the shear box apparatus will certainly be considered in the future.

- In the field, given the climatic and environmental influences, the pore water salinity can vary with time due to ion exchange. In this study, time-dependent change in salinity was not considered.
- The proposed model was influenced by electrical conductivity measurement, where only the role of NaCl was considered. However, the model can deviate from accuracy if the soil solution containsother cations such as Fe^{3+} or Fe^{2+}.
- At very high matric suctions existing under exceedingly dry conditions, the effect ofsalt crystallisation on the soil shear strength cannot be predicted by this model.

CONCLUSION

A series of direct shear box tests were carried out on a typical unsaturated saline soil (CL) subjected to different levels of osmotic suction with known values of initial matric suction. While still embracing the Mohr-Coulomb mathematical framework, this study proposed a new relationship to capture the role of osmotic suction by introducing a newparameter χ_2(i.e. as an independent term toχ_1) in the original Bishop's unsaturated shear strength model modified by Khabbaz and Khalili (1998). The following key conclusions can be drawn based on the results of this study.

- The parameter $\chi_2$representing the role of osmoticcomponent can be estimated based on the electrical conductivity ratio (ECR).The maximum value of $\chi_2$and the corresponding minimum (critical)value $ECR_c$for a given degree of saturation define the appropriate bounds of χ_2 that reaches its maximum of 0.003 when ECR_c = 900 at full-saturation (S_r= 1).

- At lower values of both osmotic suction and initial matric suction, the predicted value of χ_2 from Equation (6) agrees with the experimental resultsfor a = 0.003, b = 0.0375 and c = 2. However, at high levels of osmotic suction(i.e. π > 4500 kPa)and at high initial matric suction(i.e. s_i> 500 kPa), the model deviates from accuracy.
- The results of this study prove that for a given increase in osmotic suction, the peak shear stress can significantly increase for both the unsaturated and saturated soil specimens. For the unsaturated soil subjected to an initial matric suction of 1500 kPa, when the osmotic suction increased from 0 to 9560 kPa, the corresponding peak shear stress increased significantly by about 75% from 133 kPa to 232 kPa. For the same increase in osmotic suction, the corresponding increase in peak shear stress of saturated test specimens from 11.5 kPa to 24.9 kPa may not seem substantial at a glance, but it is noteworthy that this increase is still more than double, hence demonstrating the beneficial influence of salinity even under saturated conditions.

DATA AVAILABILITY STATEMENT

All data, models, and code generated or used during the study appear in the submitted article.

ACKNOWLEDGMENT

The authors wish to acknowledge the financial support provided by the Australian Government Research Training Program Scholarship and ARC Industry Transformation Training Centre for Advanced Rail Track Technologies (ITTC-Rail). The authors also appreciate the assistance provided by the University of Wollongong (UOW) technical staff member, Richard Berndt. The authors also acknowledge the contributions of past PhD students and Research associates at UOW who have conducted research on native

vegetationand unsaturated soil mechanics, namely Dr BehzadFatahi, Dr ShiranGunasena, Dr UdeshiniPathirage and Dr MudithaPallewatha.

REFERENCES

ABEDI-KOUPAI, J. & MEHDIZADEH, H. 2007. Estimation of osmotic suction from electrical conductivity and water content measurements in unsaturated soils. *Geotechnical Testing Journal,* 31**,** 142-148.

ADAM, I., MICHOT, D., GUERO, Y., SOUBEGA, B., MOUSSA, I., DUTIN, G. & WALTER, C. 2012. Detecting soil salinity changes in irrigated Vertisols by electrical resistivity prospection during a desalinisation experiment. *Agricultural water management,* 109**,** 1-10.

ARORA, S. 2017. Diagnostic properties and constraints of salt-affected soils. *Bioremediation of Salt Affected Soils: An Indian Perspective.* Springer.

BARBOUR, S. & FREDLUND, D. 1989. Mechanisms of osmotic flow and volume change in clay soils. *Canadian Geotechnical Journal,* 26**,** 551-562.

BISHOP, A. W. 1960. The principles of effective stress, *Norges Geotekniske Institute*.

DI MAIO, C., SANTOLI, L. & SCHIAVONE, P. 2004. Volume change behaviour of clays: the influence of mineral composition, pore fluid composition and stress state. *Mechanics of materials,* 36**,** 435-451.

DI MAIO, C. & SCARINGI, G. 2016. Shear displacements induced by decrease in pore solution concentration on a pre-existing slip surface. *Engineering geology,* 200**,** 1-9.

414 FREDLUND, D. G., RAHARDJO, H. & FREDLUND, M. D. 2012. Unsaturated soil
415 mechanics in engineering practice, *John Wiley & Sons*.

416 GALLAGE AND UCHIMURA 2015. Direct Shear Testing on Unsaturated Silty Soils to
417 Investigate the Effects of Drying and Wetting on Shear Strength Parameters at Low Suction
418 *Journal of Geotechnical and Geoenvironmental Engineering*, Vol. 142, Issue 3 (March
419 2016).

420 GARAKANI, A.A., HAERI, S.M., CHERATI, D.Y., GIVI, F.A., TADI, M.K., HASHEMI,
421 A.H., CHITI, N. AND QAHREMANI, F., 2018. Effect of road salts on the hydro-mechanical
422 behavior of unsaturated collapsible soils. *Transportation Geotechnics*, 17, pp.77-90.

423 GRAHAM, J., OSWELL, J. & GRAY, M. 1992. The effective stress concept in saturated
424 sand-clay buffer. *Canadian Geotechnical Journal,* 29**,** 1033-1043.

425 HEN-JONES, R., HUGHES, P., GLENDINNING, S., GUNN, D., CHAMBERS, J.,
426 WILKINSON, P. & UHLEMANN, S. 2014. Determination of moisture content and soil
427 suction in engineered fills using electrical resistivity. *CRC Press/Balkema*.

428 JAYATHILAKA, P., INDRARATNA, B. & HEITOR, A. 2019. Influence that Osmotic
429 Suction and Tree Roots has on the Stability of Coastal Soils. *Geotechnics for Transportation*
430 *Infrastructure.* Springer.

431 JIAO-JUN, Z., HONG-ZHANG, K. & GONDA, Y. 2007. Application of Wenner
432 configuration to estimate soil water content in pine plantations on sandy land. *Pedosphere,*
433 17**,** 801-812.

JOTISANKASA A., MAIRAING W., 2010. “Suction-monitored direct shear testing of residual soils from landslide-prone areas”, *Journal of Geotechnical and Geoenvironmental Engineering*, Vol. 136, No. 3: p. 533-537.

KHABBAZ, M. & KHALILI, N. 1998. A unique relationship for chi for the determination of the shear strength of unsaturated soils. *Geotechnique,* 48**,** 681-687.

KHALILI, N. 2018. Guidelines for the application of effective stress principle to shear strength and volume change determination in unsaturated soils. *Australian Geomechanics Journal,* 53**,** 37-47.

KHALILI, N., GEISER, F. & BLIGHT, G. 2004. Effective stress in unsaturated soils: Review with new evidence. *International journal of Geomechanics,* 4**,** 115-126.

LI, S., LI, H., XU, C.-Y., HUANG, X.-R., XIE, D.-T. & NI, J.-P. 2013. Particle interaction forces induce soil particle transport during rainfall. *Soil Science Society of America Journal,* 77**,** 1563-1571.

LIANG, Y., HILAL, N., LANGSTON, P. & STAROV, V. 2007. Interaction forces between colloidal particles in liquid: Theory and experiment. *Advances in colloid and interface science,* 134**,** 151-166.

LU, N. & LIKOS, W. J. 2006. Suction stress characteristic curve for unsaturated soil. *Journal of geotechnical and geoenvironmental engineering,* 132**,** 131-142.

MURRAY, E. J. & SIVAKUMAR, V. 2010. Unsaturated soils: a fundamental interpretation of soil behaviour, *John Wiley & Sons*.

PATHIRAGE, U., INDRARATNA, B., PALLEWATTHA, M. & HEITOR, A. 2017. A theoretical model for total suction effects by tree roots. *Environmental Geotechnics*, 1-8.

PIEGARI, E. & MAIO, R. D. 2013. Estimating soil suction from electrical resistivity. *Natural Hazards and Earth System Sciences,* 13, 2369-2379.

RAO, S. M. & THYAGARAJ, T. 2007. Swell–compression behaviour of compacted clays under chemical gradients. *Canadian geotechnical journal,* 44, 520-532.

READ, D. & CAMERON, D. 1979. Relationship between salinity and Wenner resistivity for some dryland soils. *Canadian Journal of Soil Science,* 59, 381-385.

RENGASAMY, P. 2006. World salinization with emphasis on Australia. *Journal of experimental botany,* 57, 1017-1023.

SHAH, P. H. & SINGH, D. 2004. A simple methodology for determining electrical conductivity of soils. *Journal of ASTM International,* 1, 1-11.

SHEVNIN, V., PEINADO, H., DELGADO, O. & RYJOV, A. Petrophysical and Electrical Study of Soil Properties in Sinaloa, Mexico. Near Surface 2010-16th EAGE European Meeting of Environmental and Engineering Geophysics, 2010.

TARANTINO A., TOMBOLATO S., 2005. "Coupling of hydraulic and mechanical behaviour in unsaturated compacted clay", *Geotechnique* 55 (4): p. 307–317.

TIWARI, B. & AJMERA, B. 2014. Reduction in fully softened shear strength of natural clays with NaCl leaching and its effect on slope stability. *Journal of Geotechnical and Geoenvironmental Engineering,* 141, 04014086.

VAN GENUCHTEN, M. T. 1980. A closed-form equation for predicting the hydraulic conductivity of unsaturated soils. *Soil science society of America journal,* 44**,** 892-898.

VANAPALLI, S., FREDLUND, D., PUFAHL, D. & CLIFTON, A. 1996. Model for the prediction of shear strength with respect to soil suction. *Canadian Geotechnical Journal*, 33, 379-392.

XU, Y. 2019. Peak shear strength of compacted GMZ bentonites in saline solution. *Engineering Geology,* 251**,** 93-99.

LIST OF TABLES

Table 1The osmotic suctions at different concentrations of NaCl

Concentration (mol/L)	Measured osmotic suction (kPa)
0.0	0.0
0.2	910
0.4	1790
0.6	2700
0.8	3690
1.0	4650
2.0	9560

508 Table 2 Experimental summary of peak shear stress

Matric suction (kPa)	σ'_N (kPa)	Peak shear stress (kPa)						
		π = 0 kPa	π = 910 kPa	π = 1790 kPa	π = 2700 kPa	π = 3690 kPa	π = 4650 kPa	π = 9560 kPa
0	10	11.46	11.71	12.71	13.96	15.48	17.02	24.93
	20	16.49	16.89	18.01	18.99	20.54	22.55	31.05
	40	27.29	27.69	28.54	29.79	31.09	33.79	42.56
25	10	24.62	24.97	26.12	27.42	29.32	30.92	37.99
	20	29.71	30.11	31.63	32.21	34.51	35.61	45.30
	40	40.45	40.83	41.93	42.85	44.95	46.58	56.30
100	10	47.42	47.71	49.11	51.29	53.64	55.81	65.47
	20	52.30	52.89	54.30	55.96	58.74	60.05	74.51
	40	63.24	63.60	65.43	66.95	68.69	71.99	83.35
200	10	60.58	61.33	63.26	65.70	68.39	71.92	84.98
	20	65.89	66.41	68.72	71.25	73.14	77.66	93.11
	40	76.32	76.90	79.43	80.89	83.18	87.87	103.43
500	10	85.65	86.54	90.97	94.95	100.09	105.88	129.04
	20	90.75	92.17	94.30	99.62	105.63	110.97	137.16
	40	101.46	102.63	106.04	108.99	113.91	120.57	149.33
1000	10	112.81	114.37	120.08	127.35	135.70	142.78	187.60
	20	118.00	120.08	125.66	130.99	142.94	149.74	196.51
	40	128.58	130.14	136.37	145.20	150.44	160.21	204.57
1500	10	133.10	135.47	143.55	152.41	162.42	173.77	232.05
	20	137.20	139.80	147.26	153.43	168.36	178.99	239.32
	40	148.90	150.65	158.51	167.73	182.01	190.48	245.12

509

510 LIST OF FIGURES

511 Fig. 1 Sensitivity analysis of χ_2(a) with varying a, (b) with varying b, (c) with varying S_r and
512 (d) with varying $\frac{a}{S_r^c}$

513 Fig. 2 Distribution of $\chi_{2_{max}}$ with respect to coefficient c for lower and higher degrees of
514 saturation

515 Fig.3 Distribution of critical *ECR* (ECR_c) with respect to coefficient b for different degrees of
516 saturation

517 Fig. 4 Particle size distribution of soil

518 Fig. 5 Soil water retention curve (SWRC)

519 Fig. 6 Distribution of electrical conductivity of soil specimens

520 Fig. 7 Direct shear box setup with the instrumental locations, (a) Schematic view of the shear
521 box, and (b) Images of the test setup

522 Fig. 8 Stress-strain behaviour of the saturated soil for various osmotic suctions (σ'_N = 10 kPa)

523 Fig. 9 Stress-strain behaviour of the soil under unsaturated conditions, (a) s_i = 500 kPa and
524 σ'_N = 20 kPa, (b) s_i = 1500 kPa andσ'_N= 40 kPa

525 Fig. 10 Distribution of maximum normal strain with osmotic suction for different initial
526 matric suctions (σ'_N = 10 kPa)

527 Fig. 11 Model calibration with s_i = 0 kPa, s_i = 200 kPa and s_i = 500 kPa (σ'_N = 20 kPa)

528 Fig. 12 Experimental and model prediction results of χ_2 for different initial matric suctions
529 with a = 0.003, b = 0.0375 and c = 2.0, when (a) σ_N' = 10 kPa and (b) σ_N' = 40 kPa

530 Fig.13 Distribution of experimental and model peak shear stress for different initial matric
531 suctions and saturated osmotic suction, (a) σ_N' = 10 kPa and (b) σ_N' = 40 kPa

532 Fig. 14 Variation of matric suction during shearing (σ_N' = 10 kPa and π = 0 kPa)

533

534

535

536

537

538

539

540

541

542

543

544

545

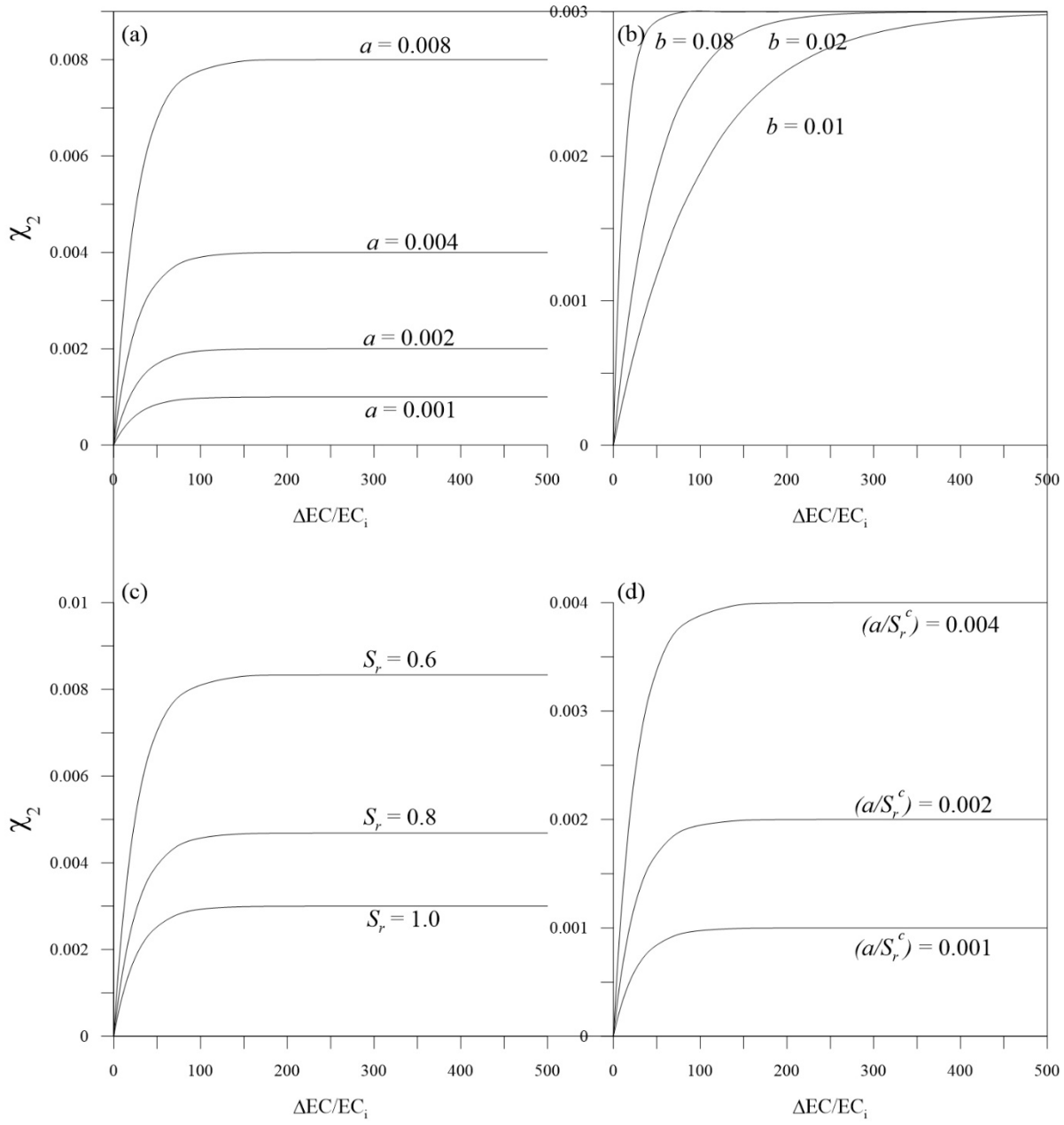

546

547

548

549

550

551

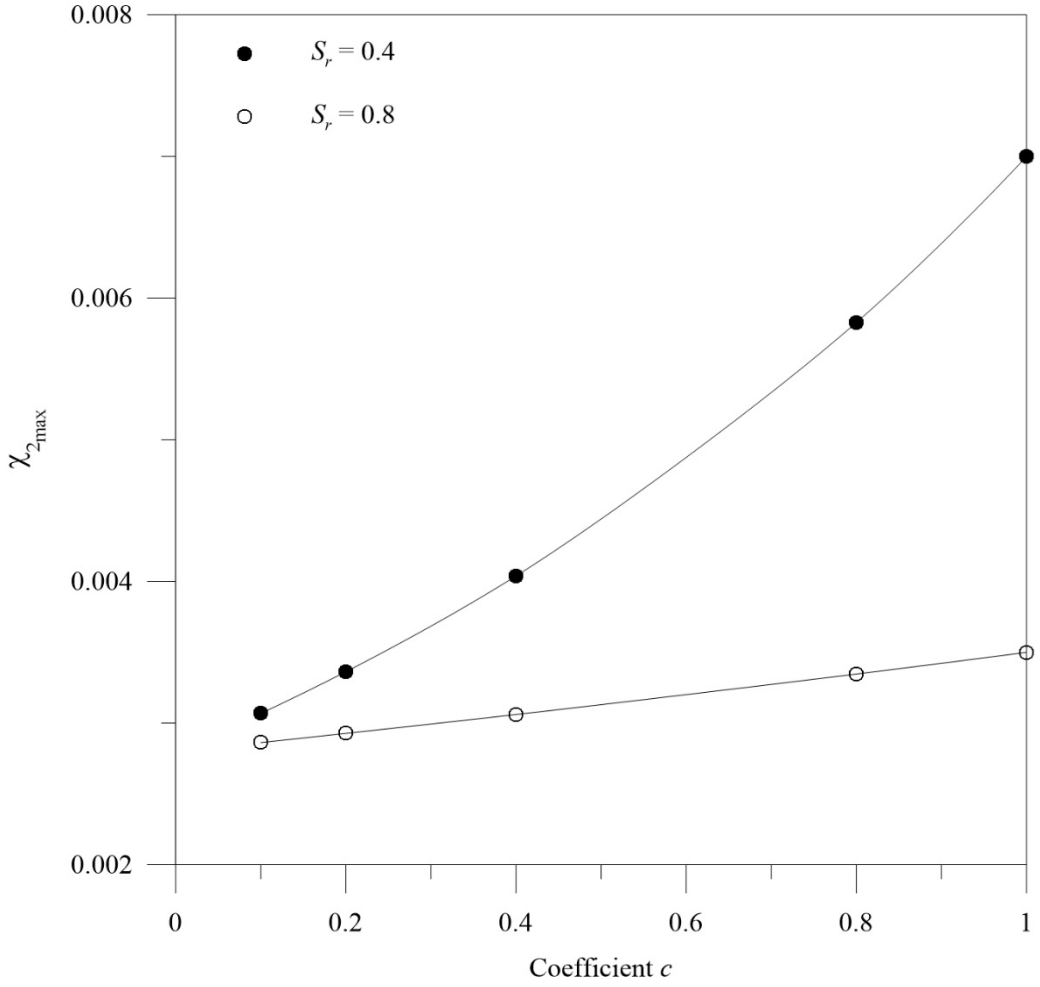

561

562

563

564

565

566

567

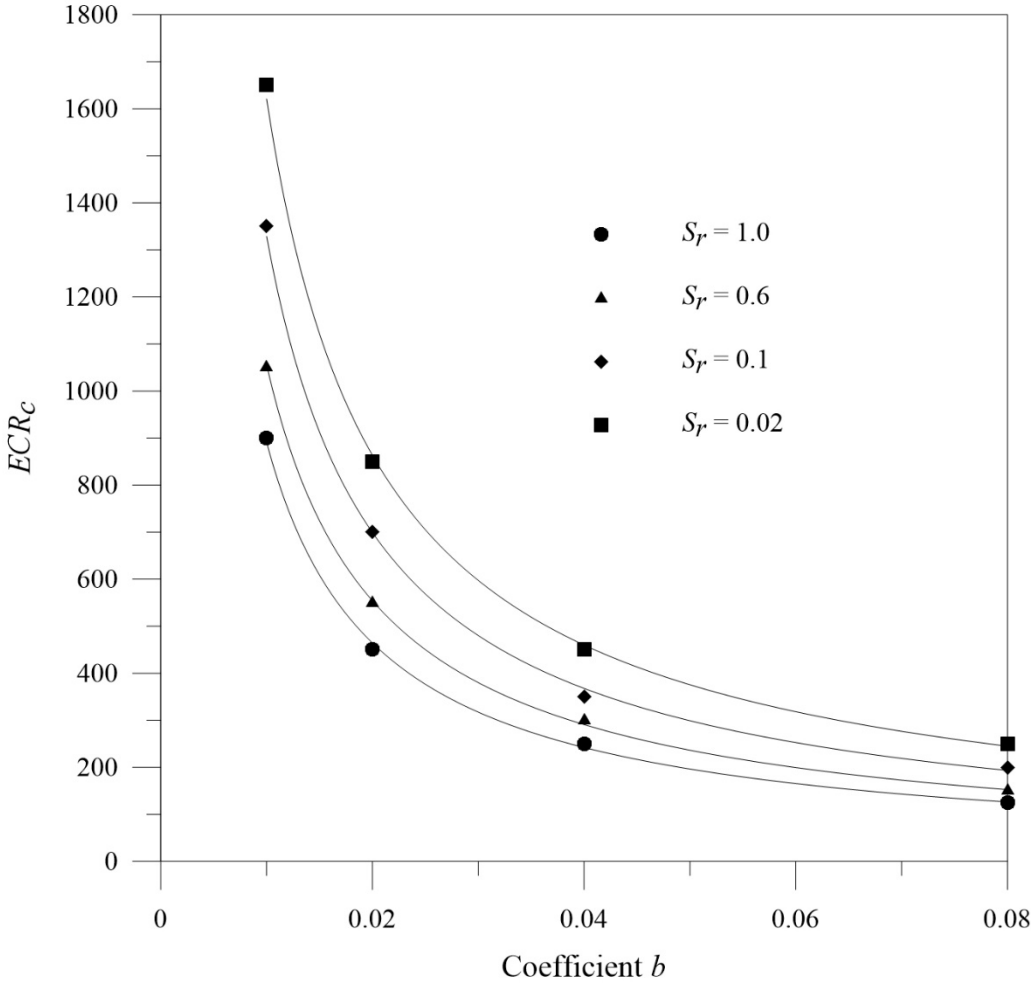

568

569

570

571

572

573

574

575

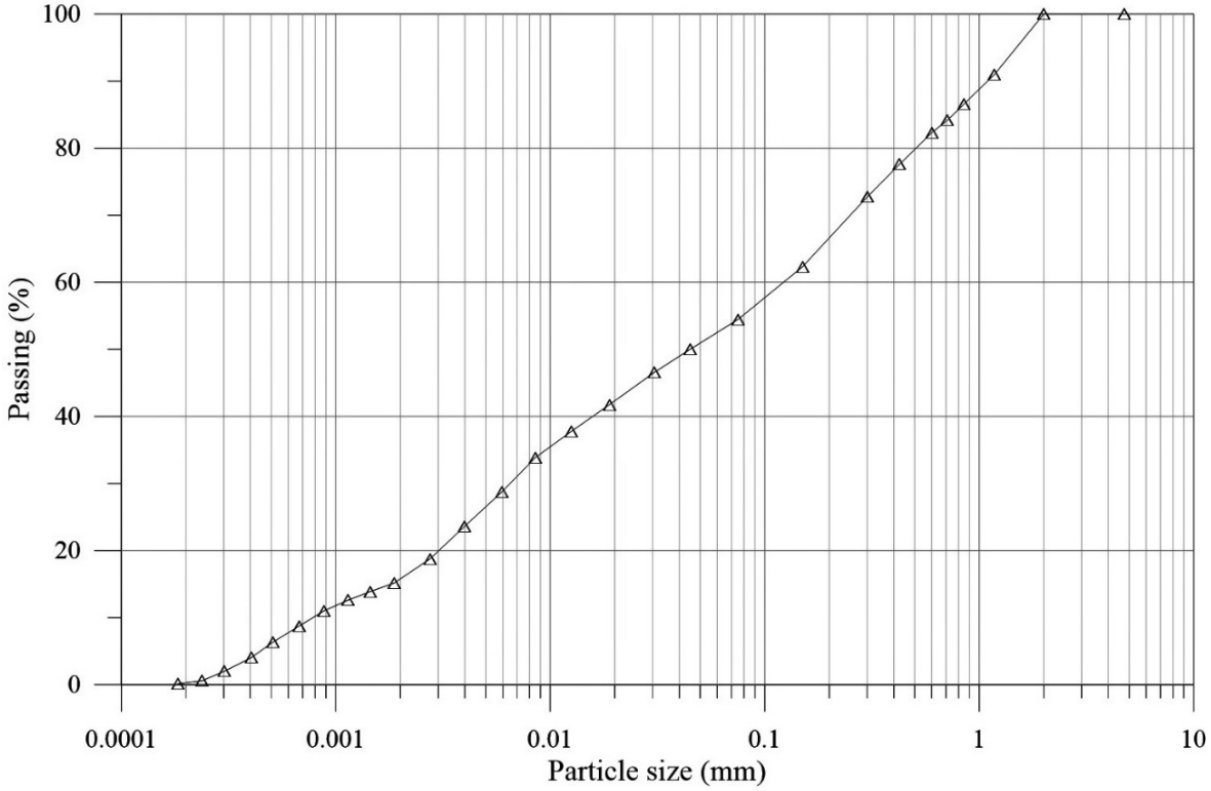

576

577

578

579

580

581

582

583

584

585

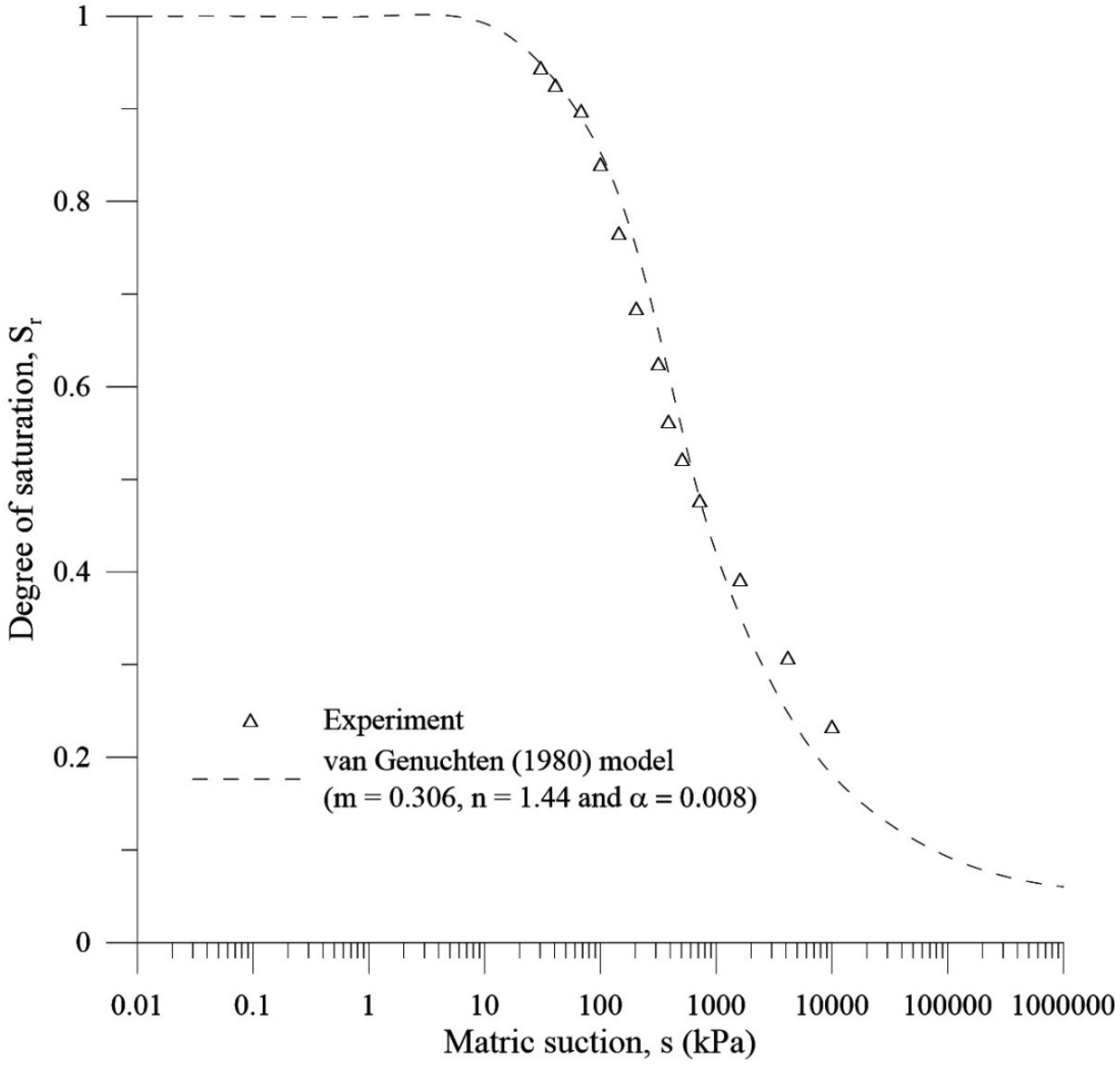

586

587

588

589

590

591

592

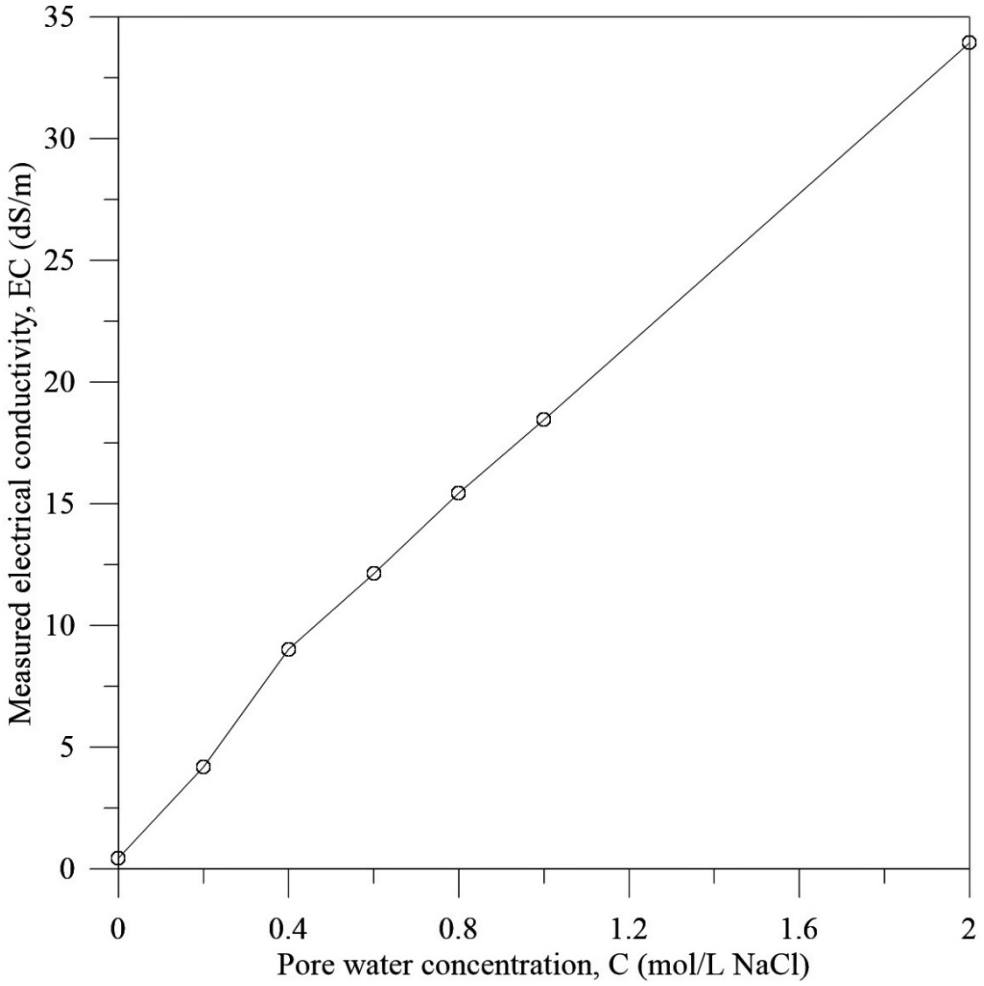

593

594

595

596

597

598

599

600

601 (a)

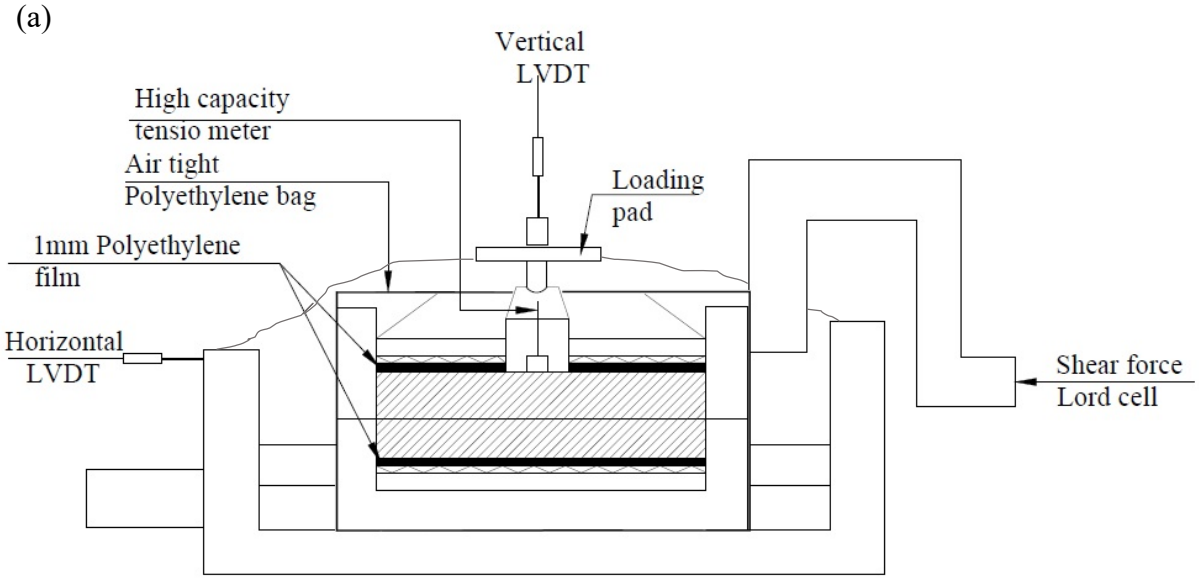

607 (b)

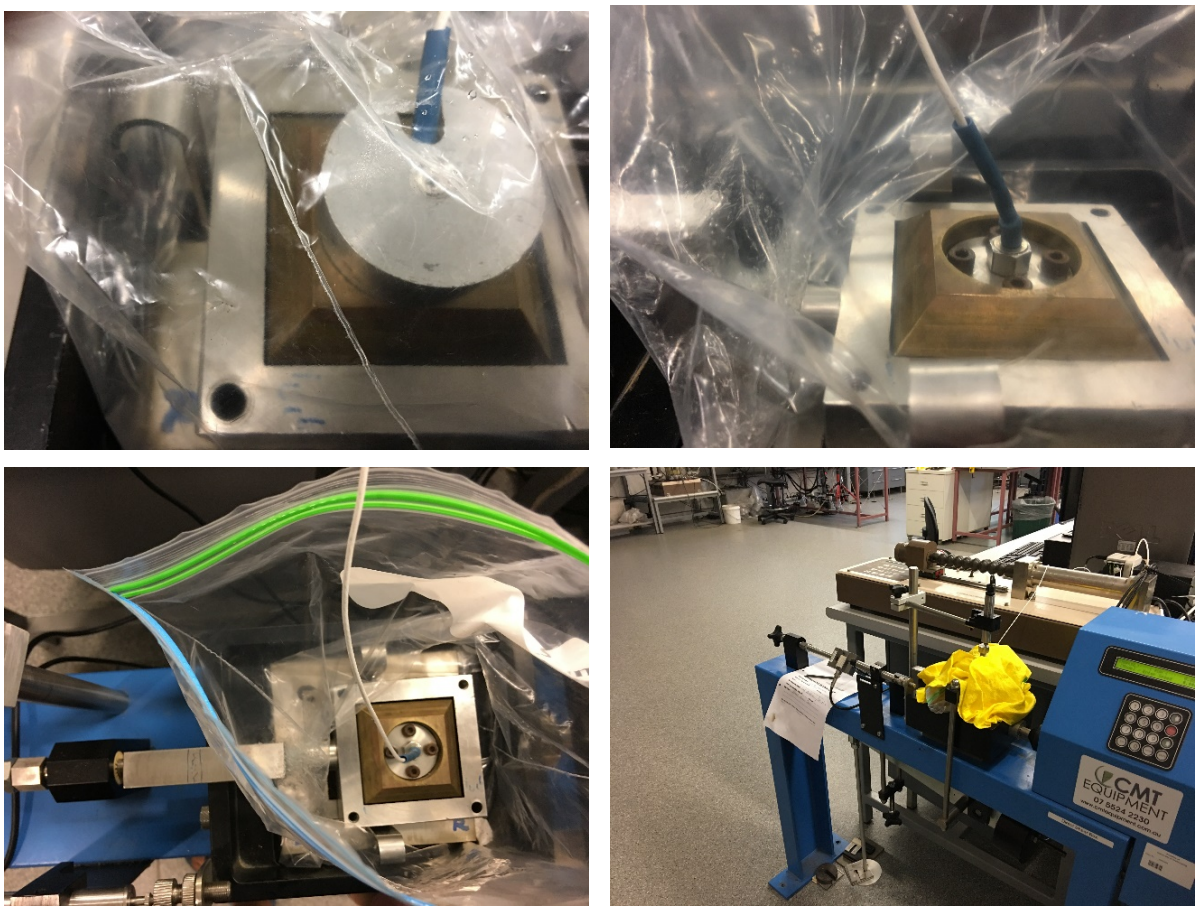

617

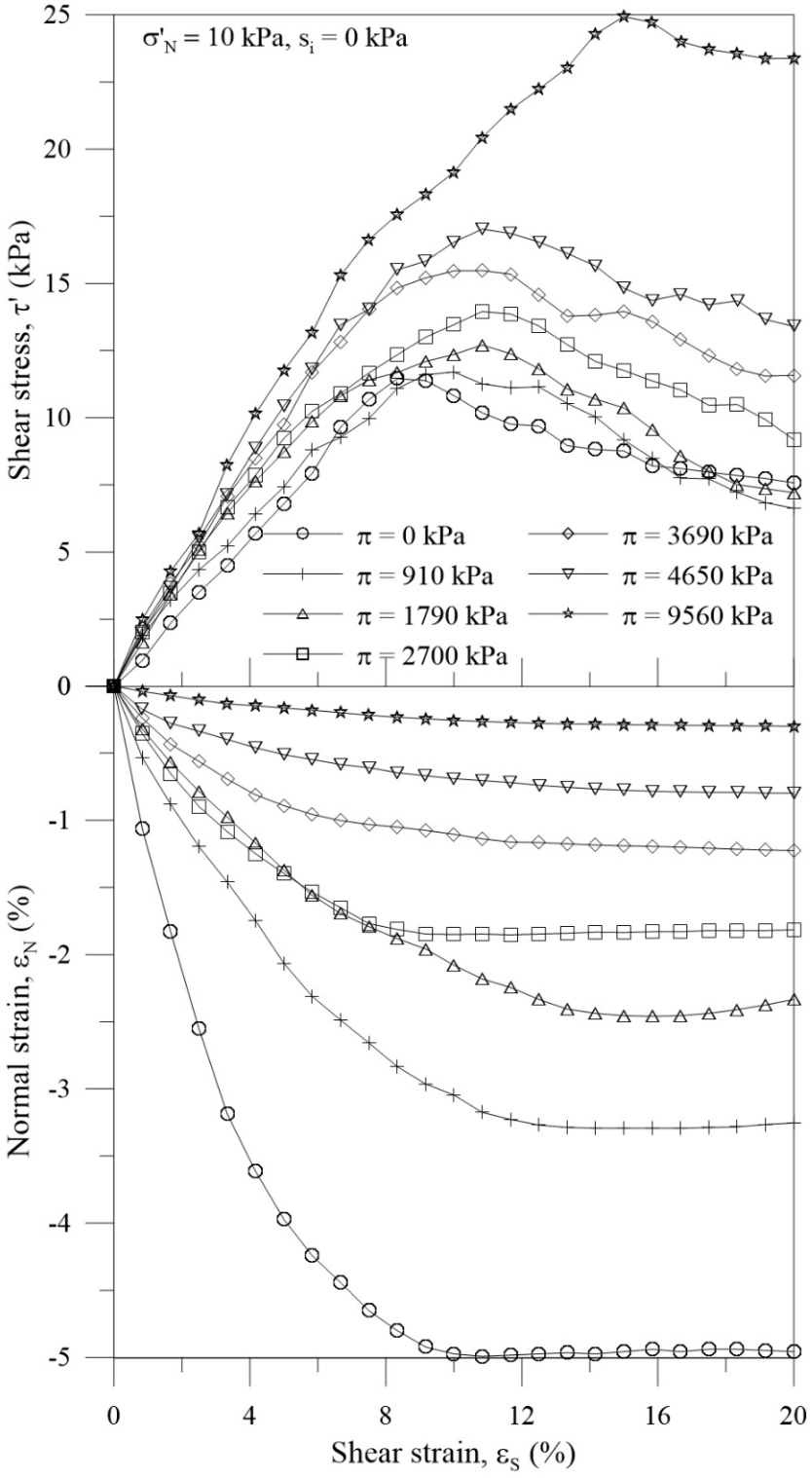
σ'N = 10 kPa, si = 0 kPa
Shear stress, τ' (kPa)
Normal strain, εN (%)
Shear strain, εS (%)
π = 0 kPa
π = 910 kPa
π = 1790 kPa
π = 2700 kPa
π = 3690 kPa
π = 4650 kPa
π = 9560 kPa
25
20
15
10
5
0
-1
-2
-3
-4
-5
0
4
8
12
16
20

618

619

620

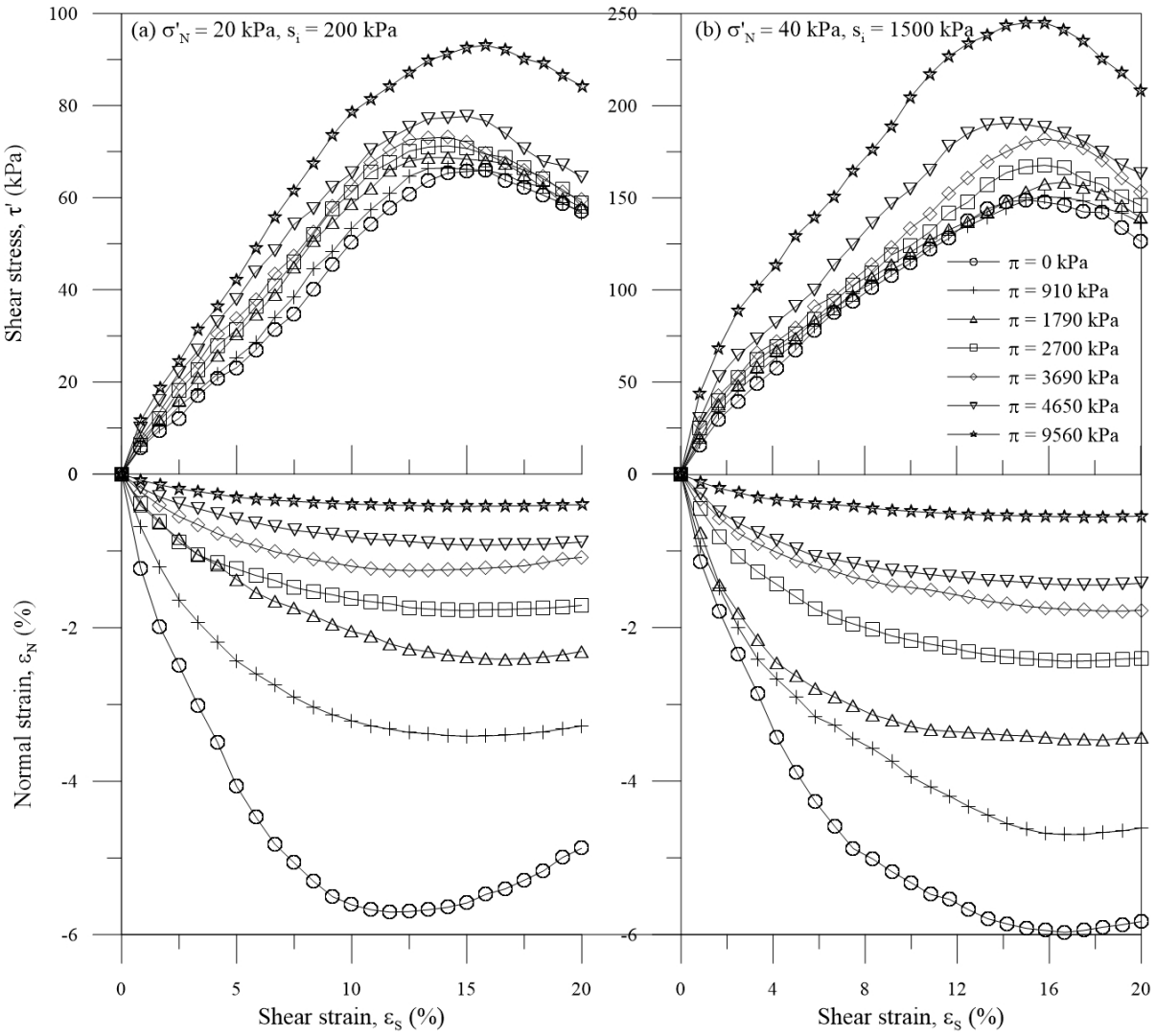

621

622

623

624

625

626

627

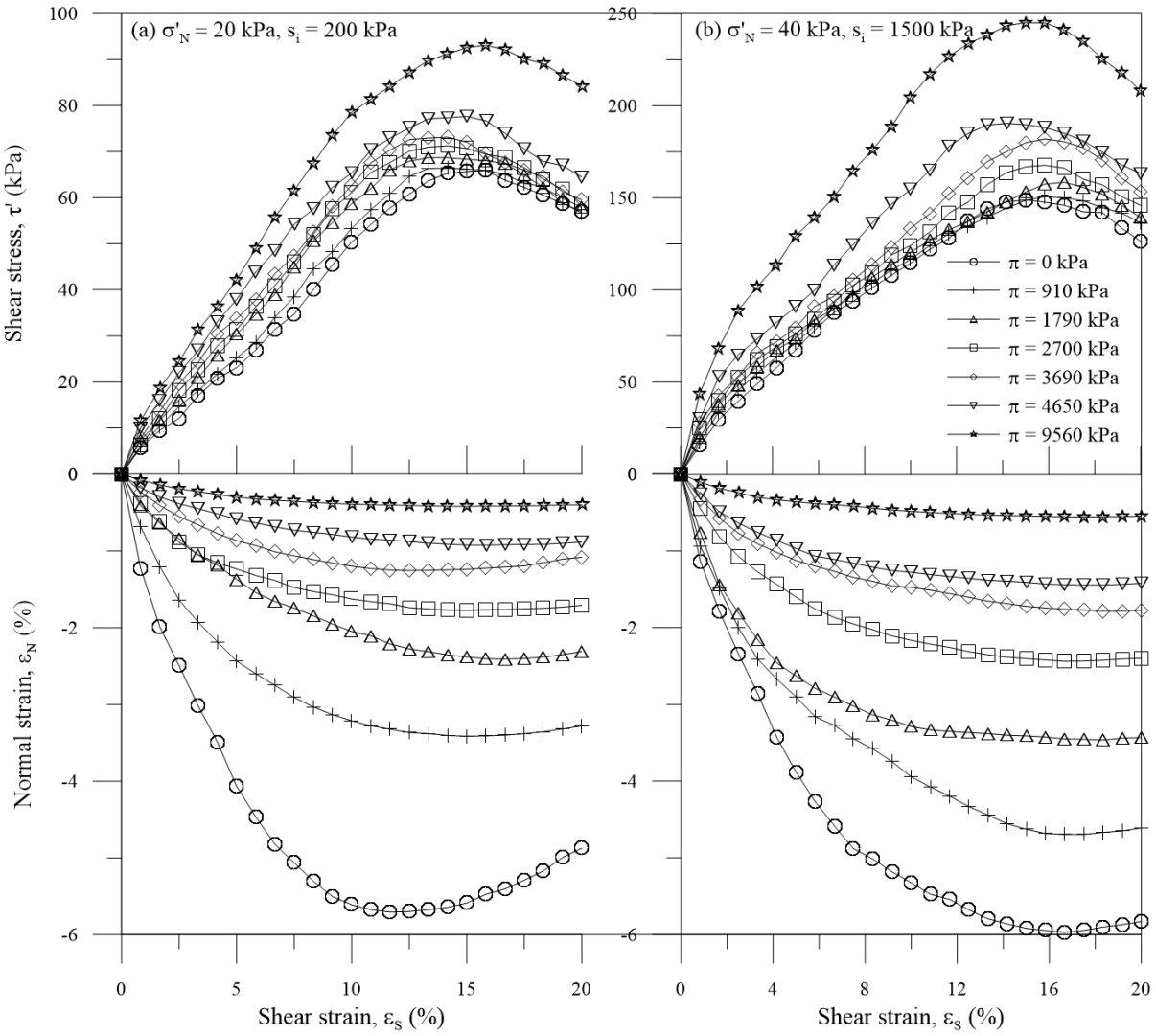

628

629

630

631

632

633

634

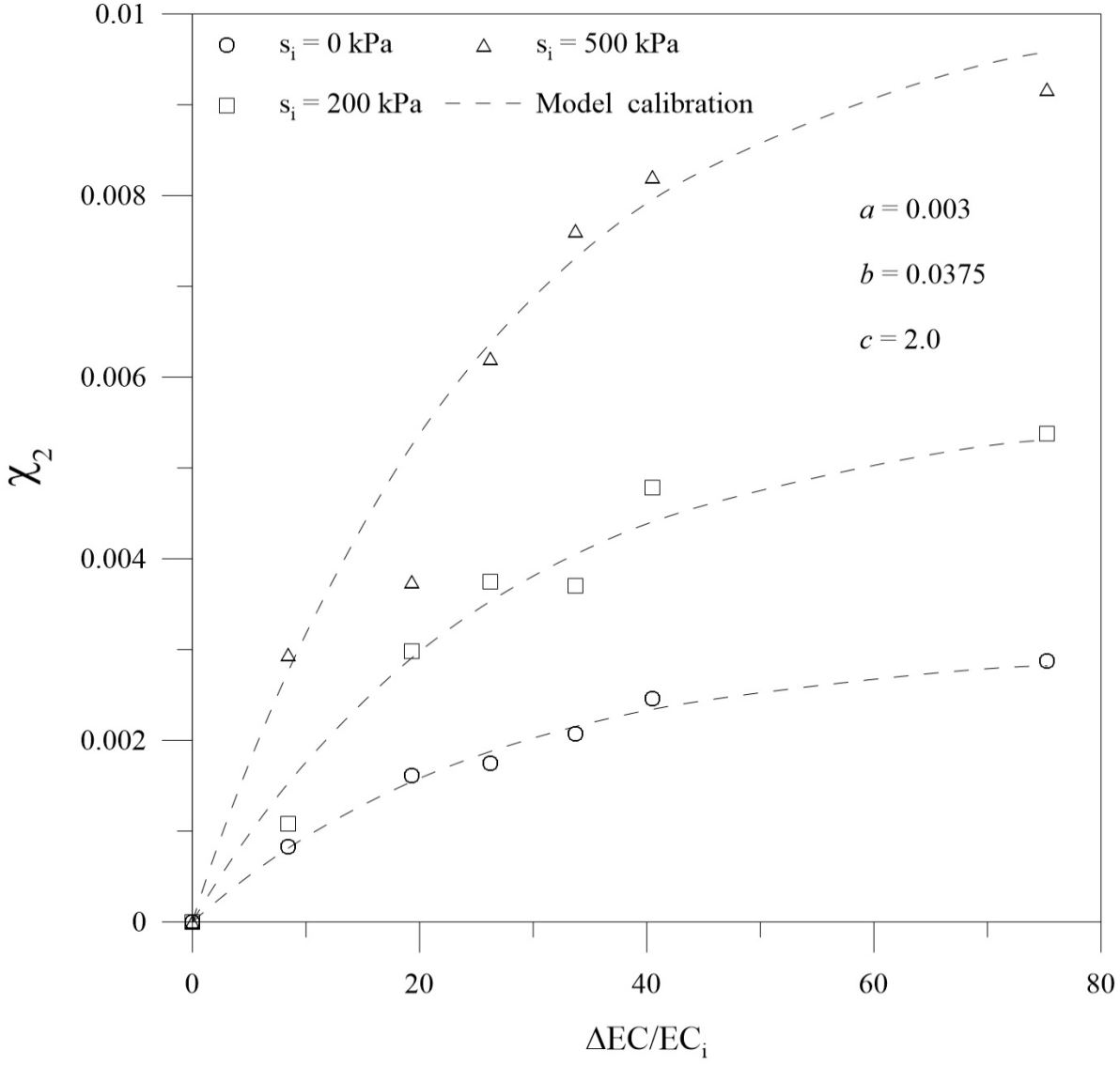

635

636

637

638

639

640

641

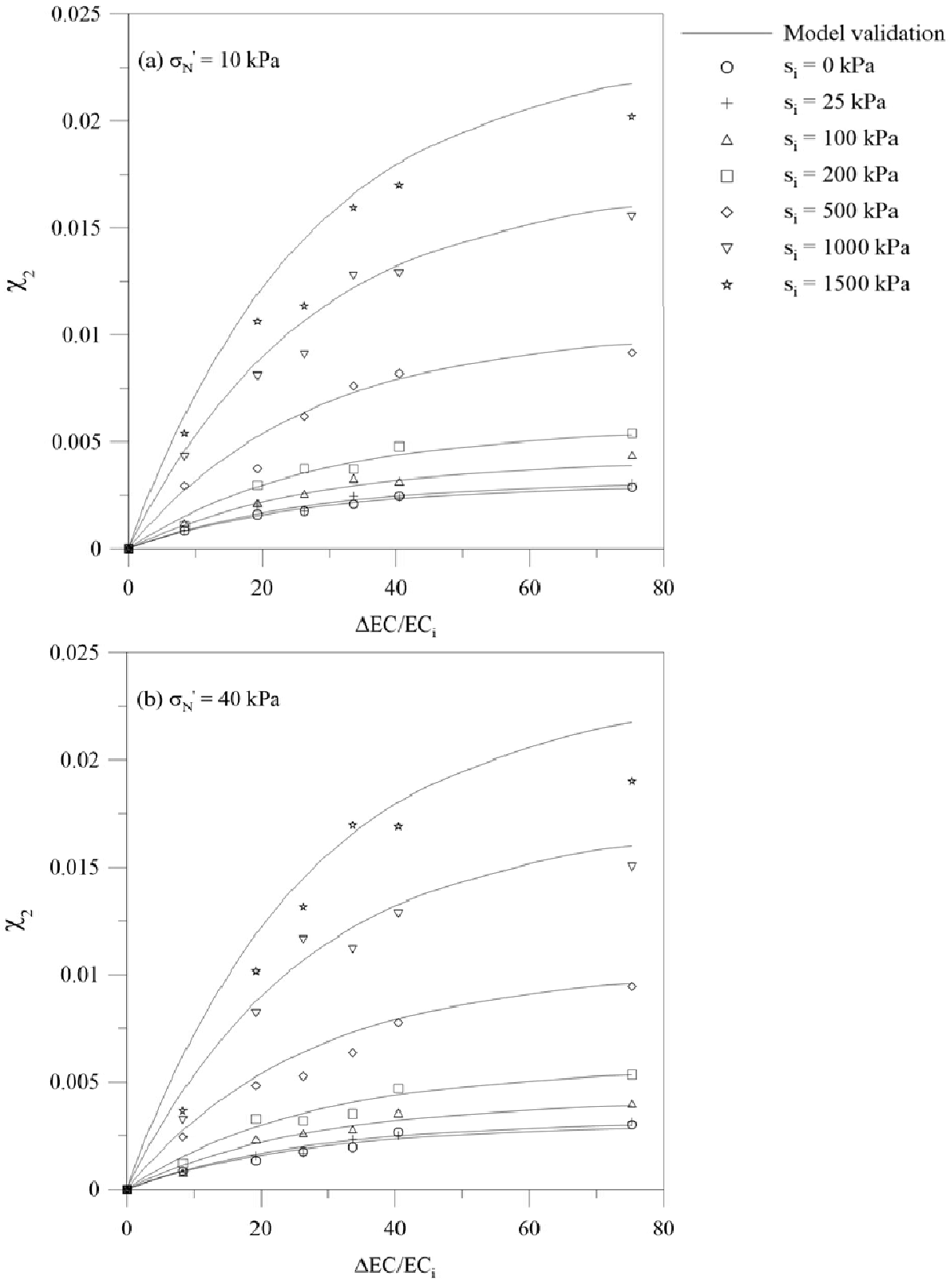
(a) σN' = 10 kPa
(b) σN' = 40 kPa
χ2
ΔEC/ECi
0.025
0.02
0.015
0.01
0.005
0
0
20
40
60
80
Model validation
si = 0 kPa
si = 25 kPa
si = 100 kPa
si = 200 kPa
si = 500 kPa
si = 1000 kPa
si = 1500 kPa

642

643

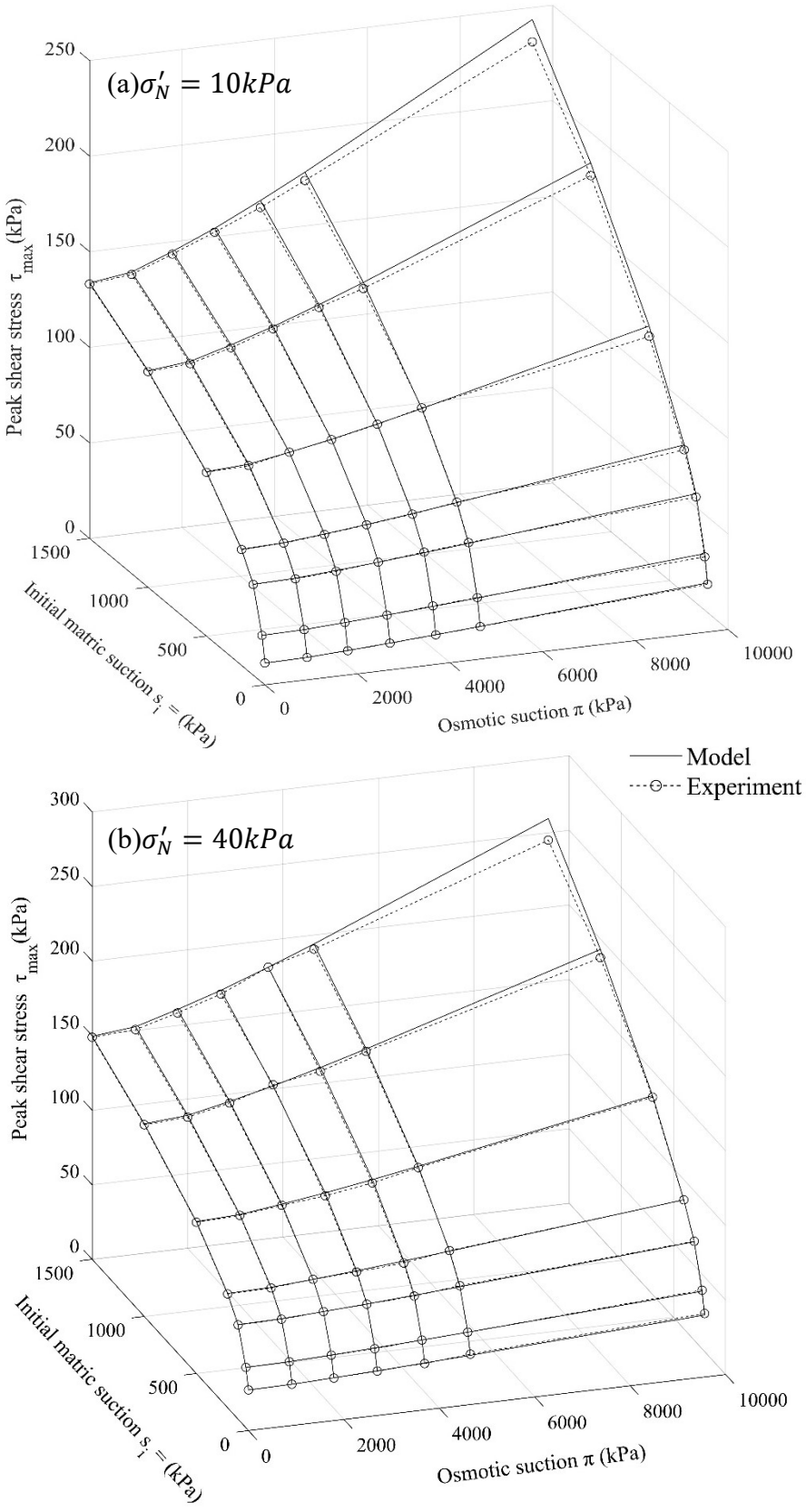
(a)$\sigma'_N = 10kPa$
Peak shear stress τ_{max} (kPa)
250
200
150
100
50
0
1500
1000
500
0
Initial matric suction s_i = (kPa)
0
2000
4000
6000
8000
10000
Osmotic suction π (kPa)
Model
Experiment
(b)$\sigma'_N = 40kPa$
Peak shear stress τ_{max} (kPa)
300
250
200
150
100
50
0
1500
1000
500
0
Initial matric suction s_i = (kPa)
0
2000
4000
6000
8000
10000
Osmotic suction π (kPa)

661

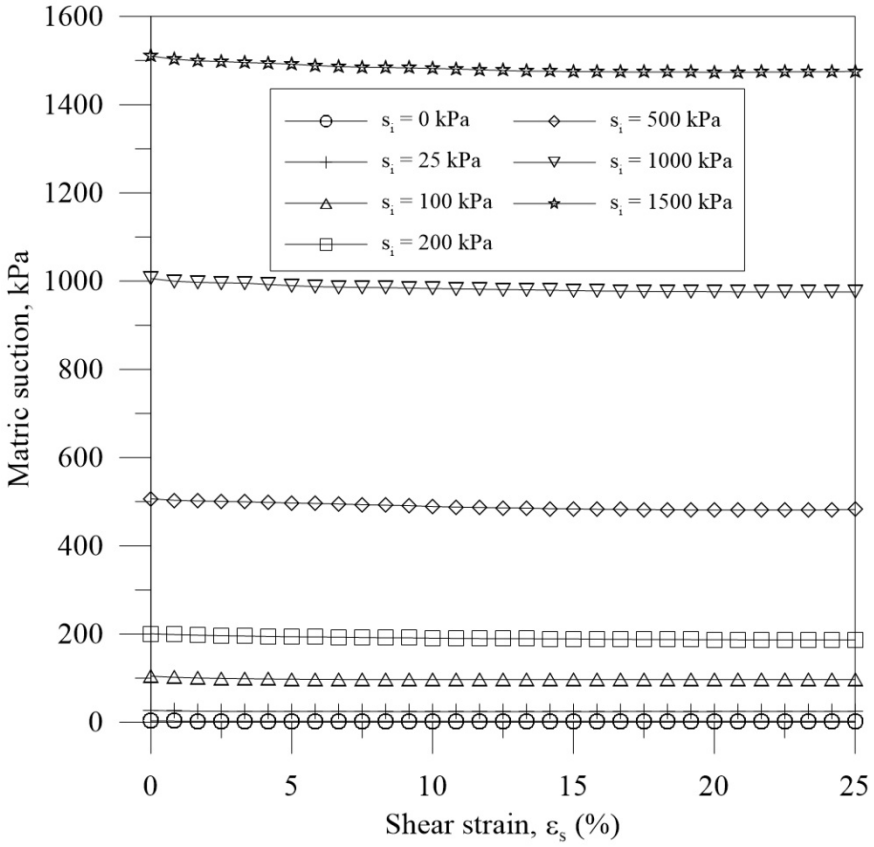
1600
1400
1200
1000
800
600
400
200
0
Matric suction, kPa
0
5
10
15
20
25
Shear strain, ε_s (%)
s_i = 0 kPa
s_i = 25 kPa
s_i = 100 kPa
s_i = 200 kPa
s_i = 500 kPa
s_i = 1000 kPa
s_i = 1500 kPa